Monte Carlo Radiative Transfer for Limb Scattered Sunlight Measurements

Seth Dueck, **Chris Roth**, Dr. Adam Bourassa, Dr. Doug Degenstein

Atmospheric Research Group, University of Saskatchewan

Simulation for Limb Scattering Geometry

Limb-viewing geometry allows observation of atmospheric radiance with a very high altitude resolution. Inversion of limb radiance measurements to atmospheric species profiles requires a *forward model* to predict radiances from "best guesses" of species profiles. Typical forward models impose *a priori* grids on diffuse light sampling points and scatter directions. Use of Monte Carlo techniques remove the constraint of discretized coordinates and allows access to data previously hidden by gridding. MC methods trade direct evaluation of an integral for probabilistic sampling of the integrand. In this case, the integrating equations of radiative transfer are solved by sampling the intensity of first-order sun-scattered light at stochastically chosen "scattering points" within the atmosphere. The contribution of light scattered at these points to observer-measured radiance is weighted according to the attenuation back to the observer along a scattering path. Convergence of the average of these weighted radiances is achieved as a large number of points are sampled.

Determining Scatter Position and Scatter Direction

Scatter Position

Transmission along a line of sight (LOS) is calculated by the Beer-Lambert Law as

$$T(s) = e^{-\int_0^s \mathrm{d}\tilde{s}\, k(\tilde{s})} \tag{1}$$

where s is path length along the LOS and $k(s)$ is optical extinction as a function of position. Consider transmission as the cumulative probability of a photon *not* interacting along the line of sight; then $(1 - T(s))$ is the cumulative probability of interaction along the LOS. This probability function is sampled by choosing a uniform random value in 0 to 1, R; inversion to a randomly chosen scatter point s_{scat} is accomplished by finding

$$s_{\mathrm{scat}} = \{s : [1 - T(s)] = R \cdot [1 - T(\mathrm{end})]\} \tag{2}$$

If the LOS passes through the atmosphere the probability of atmospheric scatter is $(1 - T(\mathrm{end}))$ and the weight of photons passing along the line must be corrected by this factor; otherwise, $T(\mathrm{end})$ represents the probability of photon ground scatter.

Scatter Direction

The *normalized phase function* $\bar{p}(\mathbf{r}, \theta)$ is the probability distribution function for an incident photon to scatter by angle θ at point $\mathbf{r}$. This can be integrated to find the *cumulative normalized phase function*

$$\bar{c}(\mathbf{r}, \theta) = \int_{\pi}^{\theta} \mathrm{d}\tilde{\theta}\, \bar{p}(\mathbf{r}, \tilde{\theta}) \tag{3}$$

which can be sampled to find a scatter direction

$$\theta_{\mathrm{scat}} = \{\theta : \bar{c}(\mathbf{r}, \theta) = R \cdot \bar{c}(\mathbf{r}, 0)\} \tag{4}$$

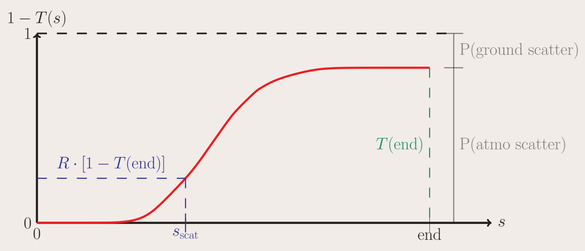

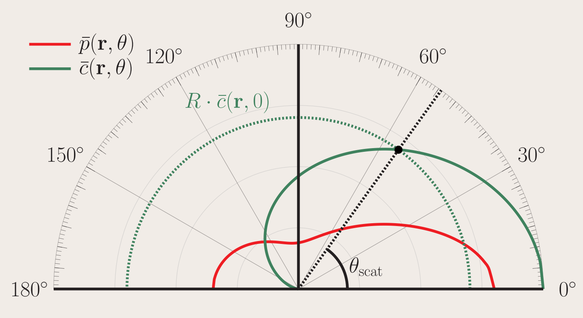

Multiple Scatter Algorithm

Transmission along the observer's line of sight is calculated and a scattering point is chosen as discussed above. All photons passing through this point will be attenuated by the transmission back to the observer and single scatter albedo at this point. Solar transmission is calculated and, having been weighted as just discussed, contributes to the observer radiance. A cumulative normalized phase function is constructed for atmospheric properties at the scatter point and is sampled to choose a new look direction relative to $\hat{\ell}$. The scattering point then effectively becomes an in-atmosphere observer: The algorithm repeats, the incoming radiance at the in-atmosphere observer contributing to the true observer's measured radiance by the appropriate weighting.

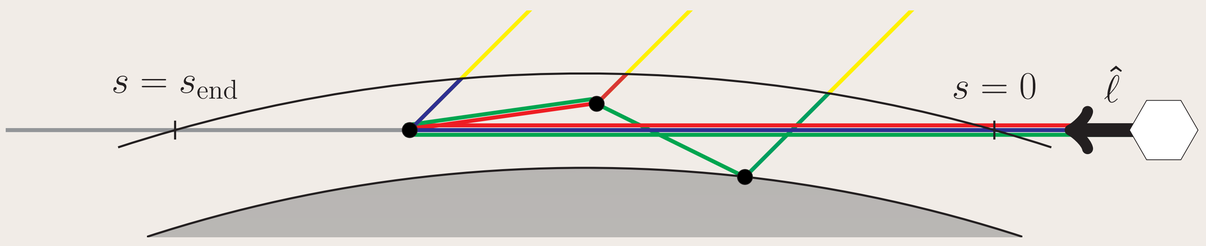

The single-path algorithm terminates once weights along the path decrease below some threshold. Many paths may be simulated by starting again from the true observer with look direction $\hat{\ell}$. The average over radiances observed along N paths converges as $\Theta(N^{-\frac{1}{2}})$.

Results

Comparisson with SKTRAN

The model is run to achieve statistical error below 0.3%; results are compared against those of the discrete SKTRAN model. Output of the two models generally agrees to within 2% except for geometries looking across the solar terminator, especially for UV wavelengths and at altitudes below 30 km. Even in extreme cases the models usually converge to within 4% for all wavelengths at altitudes above 30km, though they may differ by up to 90% of the MC value at lower altitudes.

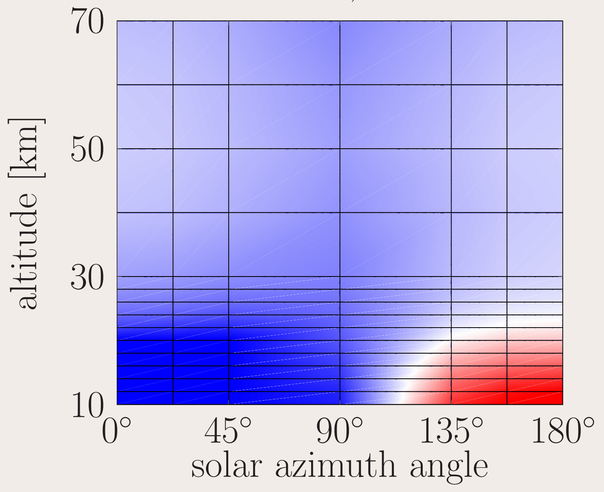

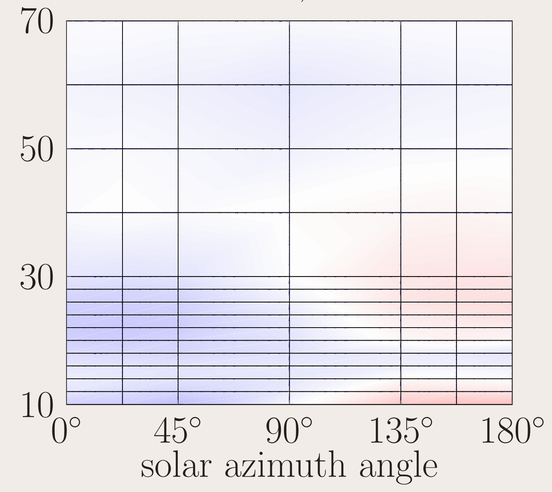

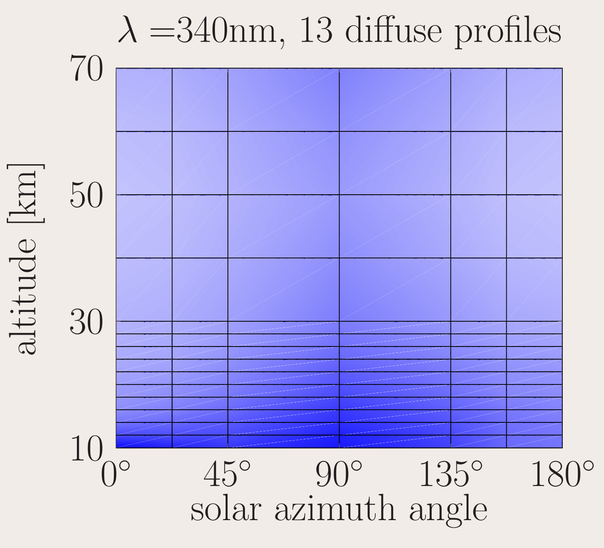

SKTRAN's performance can been improved by increasing the number of vertical profiles at which it calculates the diffuse field. The figure at left shows the difference between SKTRAN and MC with SKTRAN calculating up to 13 diffuse profiles, reducing the maximum disagreement from 48% to 7% (c.f. above left). Memory requirements and computation time required grow quickly as the number of diffuse profiles increases, however: A more sophisticated method for choosing the number and location of SKTRAN's diffuse profiles should be developed to improve performance while minimizing increase in computational burden.

Three-dimensional kernels

Three-dimensional atmospheres are easily handled in MC simulations. Kernel (Jacobian) matrices, displayed below, show the effect small-region increases in the number density of ozone and aerosol on radiance at 750 nm and 310 nm, respectively.

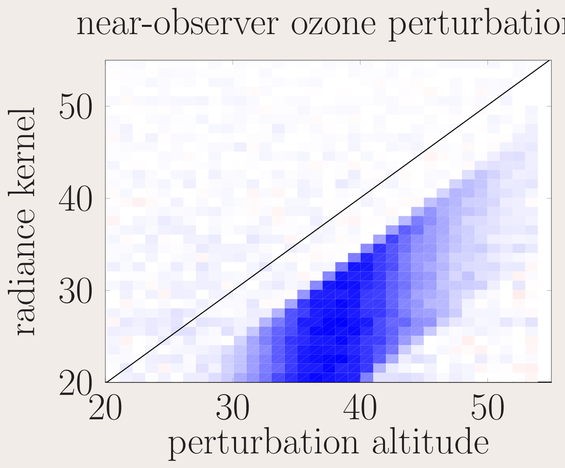

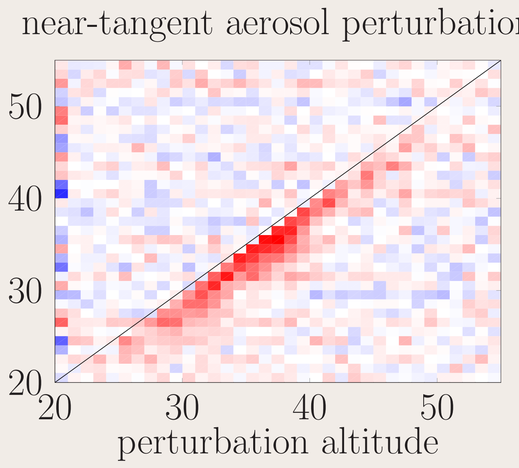

Averaging kernels

Averaging kernels describe which portions of the atmosphere contribute the most to observed radiance. These are shown on a log color scale for near-UV and red-light simulations below with the observer looking into the limb from the left of the figures. Observe that the red-light averaging kernel is symmetric about the tangent point, with large contributions coming from ground scatter and the low-atmosphere. The near-UV averaging kernel, however, is skewed strongly towards the observer. This explains the weaker agreement between MC and SKTRAN for UV wavelengths, as SKTRAN oversamples different portions of the diffuse light field depending on observer geometry and the field is highly non-symmetric at UV wavelengths.